Since January 2020 Elsevier has created a COVID-19 resource centre with free information in English and Mandarin on the novel coronavirus COVID-19. The COVID-19 resource centre is hosted on Elsevier Connect, the company's public news and information website.

Biomedicine & Pharmacotherapy 151 (2022) 113124

Contents lists available at ScienceDirect

Biomedicine & Pharmacotherapy

journal homepage: www.elsevier.com/locate/biopha

In vitro characterization of the furin inhibitor MI-1851: Albumin binding, interaction with cytochrome P450 enzymes and cytotoxicity

Erzsébet Pászti-Gere [a,*], Anna Szentkirályi-Tóth [a], Pál Szabó [b], Torsten Steinmetzer [c], Eszter Fliszár-Nyúl [d], Miklós Poór [d,e,**]

[a] Department of Pharmacology and Toxicology, University of Veterinary Medicine, Budapest, Hungary
[b] MS Metabolomics Laboratory, Center for Structural Study, Research Center for Natural Sciences, Budapest, Hungary
[c] Faculty of Pharmacy, Institute of Pharmaceutical Chemistry, Philipps University Marburg, Marburg, Germany
[d] Department of Pharmacology, Faculty of Pharmacy, University of Pécs, Pécs, Hungary
[e] Lab-on-a-Chip Research Group, János Szentágothai Research Centre, University of Pécs, Pécs, Hungary

ARTICLE INFO

Keywords:
MI-1851
Furin inhibitor
Primary human hepatocytes
CYP3A4
Human serum albumin
Cell viability

ABSTRACT

The substrate-analog furin inhibitor MI-1851 can suppress the cleavage of SARS-CoV-2 spike protein and consequently produces significant antiviral effect on infected human airway epithelial cells. In this study, the interaction of inhibitor MI-1851 was examined with human serum albumin using fluorescence spectroscopy and ultrafiltration techniques. Furthermore, the impacts of MI-1851 on human microsomal hepatic cytochrome P450 (CYP) 1A2, 2C9, 2C19, 2D6 and 3A4 activities were assessed based on fluorometric assays. The inhibitory action was also examined on human recombinant CYP3A4 enzyme and on hepatocytes. In addition, microsomal stability (60 min) and cytotoxicity were tested as well. MI-1851 showed no relevant interaction with human serum albumin and was significantly depleted by human microsomes. Furthermore, it did not inhibit CYP1A2, 2C9, 2C19 and 2D6 enzymes. In human hepatocytes, CYP3A4 was significantly suppressed by MI-1851 and weak inhibition was noticed in regard to human microsomes and human recombinant CYP3A4. Finally, MI-1851 did not impair the viability and the oxidative status of primary human hepatocytes (up to 100 μM concentration). Based on these observations, furin inhibitor MI-1851 appears to be potential drug candidates in the treatment of COVID-19, due to the involvement of furin in S protein priming and thus activation of the pandemic SARS-CoV-2.

1. Introduction

Infections with certain coronaviruses, such as severe acute respiratory syndrome coronavirus (SARS-CoV) and the Middle East respiratory syndrome coronavirus (MERS-CoV), can lead to severe respiratory diseases, while human coronavirus-229E (HcoV-229E), HcoV-HKU1, HcoV-NL63, and HcoV-0C43 cause only mild symptoms. Spike proteins (S) of SARS-CoV and MERS-CoV are cleaved by cellular serine proteases, resulting in the propagation of infectivity in the host [1,2]. Therefore, the inhibition of proteolytic S protein activity can be a useful strategy against SARS-CoV-2 infections (due to the hindrance of virus entry into the host cells) [3–10]. The activity of the membrane-associated, epithelium-derived transmembrane serine protease 2 (TMPRSS2) can be reduced by aprotinin, a broad-range inhibitor of numerous trypsin-like serine proteases. For instance, aprotinin (10 μM; 48 h post infection) decreased the virus replication *in vitro* [4]. As a result of the treatment with 3-amidinophenylalanine-derived inhibitors MI-432 and MI-1900, the viral titers were also efficiently reduced in human airway epithelial Calu-3 cells [4]. In the absence of TMPRSS2 expression (*e.g.*, in HEK293T and Vero cells), the suppression of cathepsin L by the cysteine protease inhibitor E64d could decrease infection with SARS-CoV-2 pseudoparticles [4–6]. Furthermore, the strong inhibition of SARS-CoV-2 could be achieved by nirmatrelvir, an orally available inhibitor of the viral 3CL main protease [11]. Currently, The U.S. Food and Drug Administration (FDA) has issued an emergency use authorization (EUA) for Paxlovid oral tablets (ritonavir-boosted nirmatrelvir). Nirmatrelvir suppresses the M^{PRO} viral protease-mediated cleavage of viral polyproteins, thus this orally bioavailable protease inhibitor exerts antiviral activity against SARS-CoV-2 replication [11]. Administration of nirmatrelvir can reduce the risk of hospitalization or

* Corresponding author.
** Corresponding author at: Department of Pharmacology, Faculty of Pharmacy, University of Pécs, Pécs, Hungary.
E-mail addresses: gere.erzsebet@univet.hu (E. Pászti-Gere), poor.miklos@pte.hu (M. Poór).

https://doi.org/10.1016/j.biopha.2022.113124
Received 2 April 2022; Received in revised form 7 May 2022; Accepted 10 May 2022
Available online 17 May 2022

death in people with mild-to-moderate COVID-19 (https://www.covid19treatmentguidelines.nih.gov/therapies/antiviral-therapy/r-itonavir-boosted-nirmatrelvir–paxlovid).

Moreover, targeting endosome acidification using peptide P9 or its derivatives P9R and 8P9R could interfere with the activity of cathepsin L and the latter could significantly decrease viral loads in hamsters [8,9].

Another potential pharmacological anti-SARS-CoV-2 target is furin, which belongs to the Ca^{2+}-dependent human subtilisin-like proprotein convertases. This serine protease plays an important role in the activation of numerous surface glycoproteins of pathogenic viruses [12,13]. The activation by furin is a prerequisite for fusion competence of the viruses. The SARS-CoV-2 S protein is activated by furin and by TMPRSS2 cleavage. Due to its involvement in the activation of the SARS-CoV-2 S protein, furin in particular has come into the focus as a potential antiviral target. The inhibition of the S protein cleavage by furin appears to be a suitable pharmacological intervention to inhibit the attachment of the virus to host cells (and the subsequent release of the viral genome) [10,14]. In many studies, the irreversible peptidomimetic furin inhibitor decanoyl-RVKR-chloromethyl ketone has been used to block the processing of numerous viral glycoproteins, including the S protein of SARS-CoV-2 [5–7,15]. Furthermore, the priming of the SARS-CoV-2 S protein could be also inhibited by the competitive reversible furin inhibitor MI-1851. leading to the significantly decreased viral loads in Calu-3 cells (190-fold, at 10 μM [4]). In a previous study, the binding mode of inhibitor MI-1851 to furin has been examined with crystal structure analysis, which explains its strong *in vitro* inhibitory potency ($K_i = 10.1$ pM) [16].

In this study, we assessed the *in vitro* interactions of the furin inhibitor MI-1851 with human serum albumin (HSA) as well as with cytochrome P450 (CYP) 1A2, 2C9, 2C19, 2D6 and 3A4 isoenzymes. Binding of MI-1851 to HSA and its potential displacing effects in regard to Sudlow's site I and site II ligands were examined employing fluorescence spectroscopy and ultrafiltration experiments. The effects of MI-1851 on CYP isoenzymes were also tested, including the interactions with CYP3A4 in human hepatic microsomes, hepatocytes and recombinant CYP3A4. To determine its non-cytotoxic concentrations, the impacts of inhibitor MI-1851 were also evaluated on the viability and the oxidative status of primary human hepatocytes (PHHs).

2. Materials and methods

2.1. Reagents

The furin inhibitor MI-1851 was available from the previous studies [16], its chemical structure is demonstrated in Fig. 1. Human serum albumin (HSA), racemic warfarin, racemic naproxen, CypExpress™ 3A4 Cytochrome P450 human kit, ketoconazole, testosterone and 6β-hydroxytestosterone were purchased from Merck (Darmstadt, Germany).

2.2. Interaction of inhibitor MI-1851 with HSA

The potential interaction of inhibitor MI-1851 with HSA was examined employing fluorescence quenching studies. Increasing amounts of MI-1851 (final concentrations: 0–10 μM) were added to HSA (2 μM) in phosphate-buffered saline (PBS, pH 7.4), after which the emission spectra were collected using 295 nm excitation wavelength [17,18]. Absorption spectra of MI-1851 in PBS was also recorded for the correction of the potential inner-filter effect, which was performed as it has been reported [17,18]. Changes in the emission signal of HSA were evaluated at 340 nm.

Ultrafiltration experiments, employing Sudlow's site I and site II markers (warfarin and naproxen, respectively) were performed as previously described [19,20]. Briefly, before the ultrafiltration of the samples, Amicon Ultra centrifugal filter units (Merck, Darmstadt, Germany) were washed once with water and once with PBS. Samples contained warfarin and HSA (1.0 and 5.0 μM, respectively) or naproxen and HSA (1.0 and 1.5 μM, respectively) in PBS without and with inhibitor MI-1851 (10 or 20 μM). After centrifugation (fixed angle rotor; 10 min, 7500 g, 25 °C), the concentration of site markers in the filtrate was quantified by HPLC as it has been earlier reported [19,20].

2.3. Impact of inhibitor MI-1851 on microsomal CYP activity

The Biovision CYP assays (BioVision, Inc, **Kampenhout, Belgium)** utilize non-fluorescent CYP1A2, 2C9, 2C19, 2D6 or 3A4 substrates capable of transforming into a detectable highly fluorescent metabolite. In these experiments, α-naphthoflavone (CYP1A2, 6 μM), tienilic acid (CYP2C9, 60 μM), (+)-N-3-benzylnirvanol (CYP2C19, 30 μM), quinidine (CYP2D6, 3 μM) and ketoconazole (CYP3A4, 5 μM) were used as positive control inhibitors.

Preparation of human hepatic microsomal supernatants (Gibco, Biocenter, Szeged, Hungary, protein concentration: 20 mg/mL) were carried out separately by mixing 25 μL with 2425 μL assay buffer and with 50 μL nicotinamide adenine dinucleotide phosphate (NADPH) generating system (100 ×). Aliquots of 50 μL microsomal suspensions were treated with inhibitor MI-1851 (each 20 μL, 0–250 μM), the reference inhibitors (each 20 μL; α-naphthoflavone, 30 μM; ketoconazole, 25 μM; tienilic acid, 300 μM; (+)- N-3-benzylnirvanol, 150 μM; quinidine, 15 μM) or assay buffer without test compounds (20 μL, background control) for 15 min at 37 °C (except in CYP2C19 assay, where 30 min incubation was applied). Afterwards, 30 μL of the appropriate CYP substrate/$NADP^+$ mixture was added to each well, yielding a final reaction volume of 100 μL/well.

Protein content of the microsomes obtained were analyzed using bicinchoninic acid protein assay kit (Pierce BCA kit, Thermo Fisher Scientific, Waltham, MA, US). The final microsomal protein concentration was 10 μg/well in each assay. Solvents applied (≤ 0.5% dimethylsulfoxide (DMSO) and ≤ 1% acetonitrile (ACN)) did not cause significant inhibition of CYP enzymes tested.

Fluorescence intensities were measured with a fluorometer (Victor

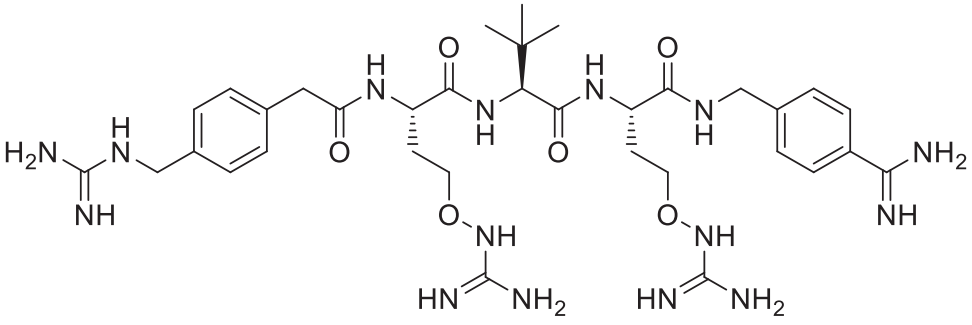

Fig. 1. Chemical structure of the furin inhibitor MI-1851.

X2 2030, Perkin Elmer, Waltham, MA, US) using $\lambda_{ex}/_{em}$= 406/468 nm for CYP1A2, $\lambda_{ex}/_{em}$= 415/502 nm for CYP2C9, $\lambda_{ex}/_{em}$= 406/468 nm for CYP2C19, $\lambda_{ex}/_{em}$= 390/468 nm for CYP2D6, and $\lambda_{ex}/_{em}$= 535/587 nm for CYP3A4 assays.

CYP3A4 assay with the human recombinant enzyme (CypExpress™ 3A4 Cytochrome P450 human kit) and with the FDA-recommended substrate testosterone as well as the quantification of the substrate and the product (6β-hydroxytestosterone) were performed as described in our recent study [21].

2.4. Depletion studies with UPLC-MS/MS

Human liver microsomes (Primacyt, Schwerin, Germany, 10 mg/mL) were treated with inhibitor MI-1851 (50 μM) for 60 min. The final protein concentrations were 0.7 mg/mL in each assay. The reaction buffer (100 mM phosphate buffer, pH 7.4) contained NADPH (1 mM), $MgCl_2$ (5 mM), glucose-6-phosphate (G6P, 10 mM) and glucose-6-phosphate dehydrogenase (G6PD, 2 IU/mL). The reaction was stopped with two-fold volume of ice-cold ACN, after which samples were centrifuged for 10 min at 10,000 g at room temperature, then the supernatants were directly analyzed.

Quantitation of the inhibitor MI-1851 was performed on a Sciex X500B Q-TOF mass spectrometer (Sciex, Framingham, MA) coupled with an Agilent 1200 HPLC system. Zorbax RX-Sil (250 ×4.6 mm, 5 μm) HPLC column was applied for the separation. Water and ACN, both containing 0.1% formic acid, were used as mobile phases A and B, respectively. Inverse gradient was applied where the water is the stronger eluent. A 5-μL aliquot of protein-precipitated and centrifuged sample was injected. The MS detection was performed in TOF mode (spray voltage: 5500 V; nebulizer gas (GS1): 40 arbitrary unit (au); drying gas (GS2): 45 au; curtain gas: 40 au; source temperature: 500 °C; declustering potential: 80 V; mass range: 120–1000 Da; accumulation time: 0.5 s) with 15 min run time. The resolution of the MS was above 30,000 for the entire mass range. The [M+ 3 H]3 + ion (256.8173) was selected for the quantitation with mass window of 0.02 Da.

2.5. Cell culture and treatment of PHHs with inhibitor MI-1851

Cryopreserved PHHs were purchased from Primacyt (Schwerin, Germany). Hepatocytes were thawed using human cryopreserved hepatocyte recovery medium (Lonza, Biocenter Ltd., Szeged, Hungary) and cells were centrifuged (10 min, 100 g, 20 °C) to remove supernatants. Cells were incubated with 5% fetal bovine serum (FBS)-containing plating medium for 6 h, then with FBS-free medium (both media were obtained from Lonza, Biocenter Ltd., Szeged, Hungary) on collagen-coated membrane inserts (Costar Transwell-COL PTFE permeable supports, 6.5 mm inserts, 0.4 μm pore size, 24-well plate, Corning Incorporated, Kennebunk ME, US) for CYP and Amplex red assays and on 96-well plates (Corning Costar Transwell, Merck, Darmstadt, Germany) for MTS investigations. Maintenance medium without FBS was replaced every 24 h and the cells were incubated at 37 °C with 5% CO_2.

Stock solution of MI-1851 (10 mM) was prepared in DMSO and kept at − 20 °C. Before treatment, PHHs were washed twice with plain (serum-free) medium. The solutions of the inhibitor were prepared freshly from the stock solutions prior to each experiment. After the treatment of cells with the inhibitor for 2 h (during CYP assays) or for 24 h (during MTS and Amplex red studies), cells were subjected to the subsequent procedures.

2.6. MTS assay

The assay is based on the ability of living cells to reduce the MTS tetrazolium compound to a formazan dye. The reduction is carried out by an NAD(P)H-dependent dehydrogenase in metabolically active cells. The assay was performed with three parallels at each concentration. The PHHs were placed onto 96-well plates and incubated for 24 h with MI-1851 (0, 10, 20, 50 and 100 μM). Then the medium was removed and cells were washed three times with PBS. CellTiter96 Aqueous One Solution (20 μL/well; Promega Corporation, Madison, WI, US) in phenol red-free Williams E medium (100 μL/well; purchased from Invitrogen, Thermo Fisher Scientific, Waltham, MA, US) were placed into a 96-well plate. After 2 h incubation (in a 5% CO_2 incubator), cell viability was evaluated based on the absorbance detected at 490 nm with an EZ Read Biochrom 400 microplate reader (Biochrom, Cambridge, UK).

2.7. Extracellular H_2O_2 measurement by the amplex red method

The changes in the extracellular H_2O_2 levels in cell supernatants were detected using the Amplex Red Hydrogen Peroxide Assay Kit (Invitrogen, Molecular Probes) in a 96-well plate. In the presence of horseradish peroxidase (HRP), Amplex Red reagent reacts with H_2O_2 (in 1:1 stoichiometry) to produce a red fluorescent product called resorufin. Following the treatment of PHHs with inhibitor MI-1851 (100 μM) for 24 h, a 50 μL aliquot of the cell free supernatant was collected and mixed with 50 μL of Amplex Red working solution in each well, then incubated for 30 min. Fluorescence intensities were measured with a fluorimeter (Victor X2 2030, Perkin Elmer, Waltham, MA, US) using 560 nm excitation and 590 nm emission wavelengths.

2.8. CYP1A2 and CYP3A4 luminescent method in PHHs

For the measurements of CYP1A2 and CYP3A4 activities, PHHs were grown on 24-well collagen-coated membrane inserts (Costar Transwell-PTFE membrane, 6.5 mm, pore size: 0.4 μm, Corning Incorporated, Kennebunk, ME, US). The hepatocytes were treated with MI-1851 (0, 10, 20, 50 and 100 μM) or the positive control inhibitors (alpha-naphthoflavone, 10 μM, CYP1A2; ketoconazole, 10 μM, CYP3A4). Effects of MI-1851 on CYP1A2 and CYP3A4 activities were determined using P450-Glo CYP450 Assays employing luciferin 1A2 or luciferin IPA (Promega, Madison, Wisconsin, US), according to the manufacturer's instructions.

2.9. Statistical analyses

For statistical evaluation R 2.11.1 software package (2010) was applied. Differences between absolute means were evaluated by one-way analysis of variance (one-way ANOVA) with post-hoc Tukey test (* $p < 0.05$, ** $p < 0.01$, *** $p < 0.001$), where data were of normal distribution and homogeneity of variances was confirmed.

3. Results

3.1. Testing the HSA binding of MI-1851

In fluorescence quenching studies, MI-1851 did not affect ($p > 0.05$) the emission signal of the protein at 340 nm (Fig. 2A and B). Since the interaction of ligand molecules with HSA causes a partial decrease in the emission signal of Trp214 in albumin, it is reasonable to hypothesize that MI-1851 does not interact with the protein or they form only poorly stable complexes [17,18].

To confirm these results, additional ultrafiltration experiments were performed. HSA is a large macromolecule (66.5 kDa), therefore, albumin and albumin-bound ligands cannot pass through the filter unit with 30 kDa molecular weight cut-off. Thus, for example, the displacement of a site marker from HSA leads to its higher concentration in the filtrate. Inhibitor MI-1851 did not affect significantly ($p > 0.05$) the filtered fractions of warfarin and naproxen, suggesting that it does not affect the albumin binding of site I and site II ligands (Fig. 2C and D) [19,20].

3.2. Effects of MI-1851 on CYP activities

First, we tested the impact of MI-1851 (50 μM) on CYP isoenzymes in

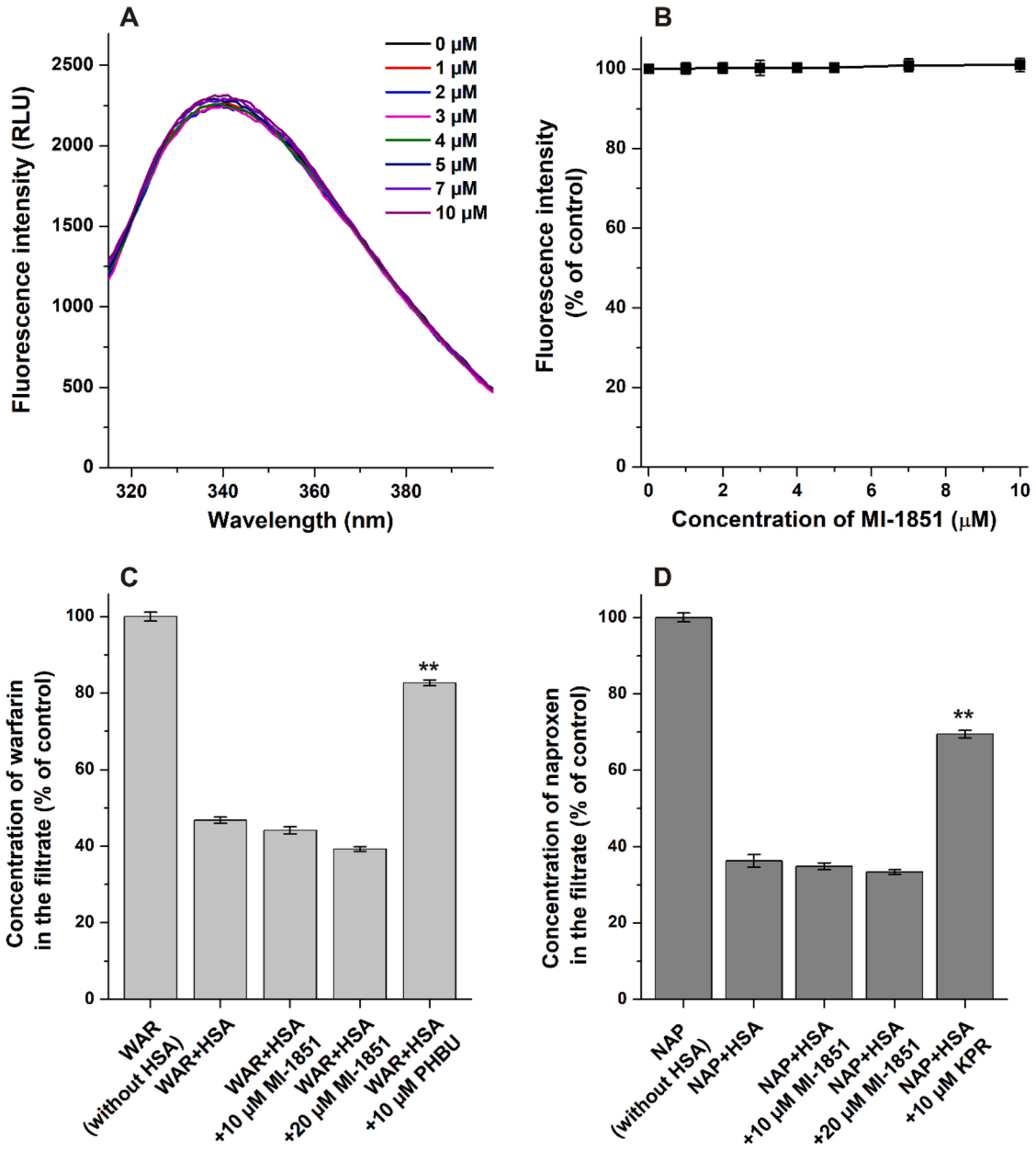

Fig. 2. Testing the interactions of MI-1851 with HSA. MI-1851 did not affect significantly ($p > 0.05$) the emission signal of HSA and the albumin binding of site I and II markers. Mean ± SEM values are demonstrated (n = 3). (A) Fluorescence emission spectra of HSA (2 μM) in the presence of increasing concentrations of inhibitor MI-1851 (0–10 μM) in PBS (pH 7.4; $\lambda_{ex} = 295$ nm). (B) Effect of MI-1851 on the relative fluorescence of HSA at 340 nm ($\lambda_{ex} = 295$ nm). (C) Influence of MI-1851 (10 or 20 μM) and the positive control phenylbutazone (PHBU, 10 μM) on the filtered fraction of warfarin (WAR). (D) Impact of MI-1851 (10 or 20 μM) and the positive control ketoprofen (KPR, 10 μM) on the filtered fraction of naproxen (NAP). Relative changes in the filtered fractions of site markers were compared to the filtered fraction determined without HSA (100%). The positive controls PHBU and KPR caused significant (**$p < 0.01$) displacement in the ultrafiltration experiments.

human microsomes. The positive controls, α-naphthoflavone, tienilic acid, (+)-N-3 benzylnirvanol and quinidine caused significant inhibition of CYP1A2 (***$p < 0.001$), CYP2C9 (***$p < 0.001$), CYP2C19 (*$p = 0.041$) and CYP2D6 (**$p = 0.007$), respectively. However, MI-1851 did not affect human microsomal CYP1A2, 2C9, 2C19 and 2D6 activities (Fig. 3A-D).

The inhibitory action of MI-1851 was also tested on human recombinant CYP3A4, employing the FDA-recommended substrate testosterone. MI-1851 caused weak, but statistically significant decrease in the CYP3A4-catalyzed 6β-hydroxytestosterone formation (*$p = 0.035$ at 20 μM; Fig. 4A), and it also showed slight but statistically significant inhibitory effect on the human microsomal CYP3A4 isoenzyme in the fluorescent assay (*$p = 0.049$ at 20 μM; Fig. 4B).

3.3. Determination of depletion percentage values of MI-1851 in microsomal stability assays

Based on the 60 min microsomal stability data, MI-1851 is partly decomposed during the exposure to hepatic microsomal CYP isoenzymes (Fig. 5). A time-dependent decrease in the concentration of MI-1851 was observed, the depletion percentage values were 7.6%, 12.1% and 45.7% after 5 min, 10 min and 60 min incubations, respectively.

3.4. Assessment of cell viability and extracellular H_2O_2 production

To evaluate the viability of the PHHs after 24 h treatment with MI-1851 (0, 10, 20, 50 and 100 μM), MTS assay was applied. Our results

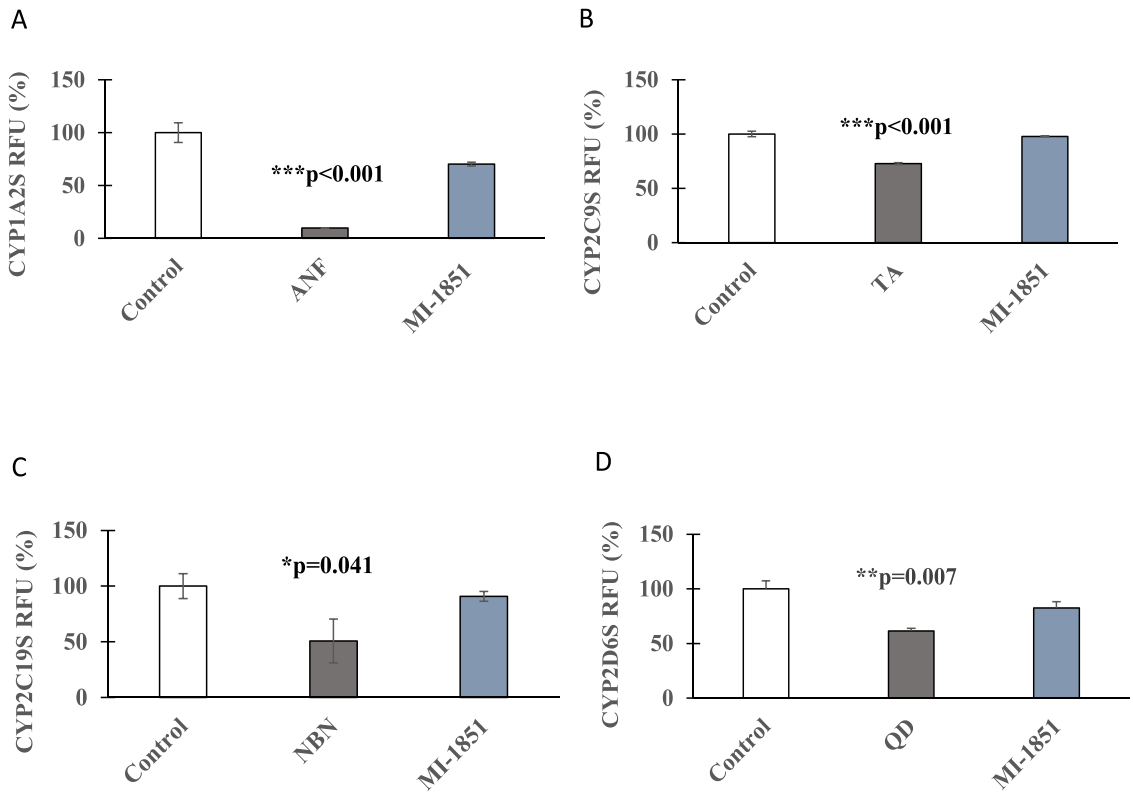

Fig. 3. Interactions of MI-1851 with CYP (1A2, 2C9, 2C19 and 2D6) isoenzymes. Impacts of inhibitor MI-1851 (50 μM) on CYP1A2 (A), CYP2C9 (B), CYP2C19 (C) and CYP2D6 (D) activities. Under the applied conditions, MI-1851 has only negligible effects on these CYP enzymes. In contrast, α-naphthoflavone (ANF, 6 μM; CYP1A2), tienilic acid (TA, 60 μM; CYP2C9), (+)-N-3 benzylnirvanol (NBN, 30 μM; CYP2C19) and quinidine (QD, 3 μM; CYP2D6) caused significant inhibition (***$p < 0.001$, ***$p < 0.001$, *$p = 0.041$ and **$p = 0.007$, respectively). Mean relative fluorescence intensities (RFU%) of relevant CYP substrates (S) ± SEM are presented ($n = 3$ or 4).

demonstrate that MI-1851 did not alter ($p > 0.05$) the viability of PHHs even at 100 μM concentration (Fig. 6).

To assess the impact of MI-1851 on H_2O_2 production, PHHs were incubated with the inhibitor at a non-cytotoxic concentration of 100 μM for 24 h. Then, the cell free supernatants were transferred to a 96-well plate and mixed with a Amplex Red working solution. Based on the fluorescent measurements, MI-1851 did not influence the production of the extracellular H_2O_2 ($p > 0.05$; Fig. 7). Thus, the extracellular redox status was maintained in PHHs exposed to this furin inhibitor.

3.5. Effects of MI-1851 on CYP1A2 and CYP3A4 in PHHs

Human PHHs were treated with the furin inhibitor MI-1851 (0, 10, 20, 50 and 100 μM) for 2 h. Based on chemiluminescent data, the activity of CYP1A2 did not change after the treatment ($p > 0.05$; Fig. 8A). However, MI-1851 at 20 μM, 50 μM and 100 μM significantly decreased CYP3A4 activity in PHHs (*$p = 0.023$, **$p = 0.001$ and *** $p < 0.001$, respectively) (Fig. 8B).

4. Discussion

SARS-CoV-2 S protein has different furin and TMPRSS2 cleavage sites, which cannot replace each other in S protein processing. It was also confirmed that the suppression of TMPRSS2 by aprotinin, and the synthetic inhibitors MI-432 and MI-1900 inhibit viral replication in Calu-3 cells infected with SARS-CoV-2 at MOI 0.001 for 90 min [4]. In the frame of *in vitro* studies of 3-amidinophenylalanine (Phe(3-Am))-derived TMPRSS2 inhibitors, it was demonstrated that MI-1900 and its structural analog MI-1907 (up to 50 μM) did not cause damage to human intestinal epithelial cells and PHHs (based on 24 h cytotoxicity assays). Furthermore, four Phe(3-Am) derivatives (MI-432, MI-463, MI-482 and MI-1900) appeared to be potent inhibitors of CYP3A4 at the nanomolar or low micromolar range in microsomal and recombinant enzyme experiments [21,22].

As it has been reported, a single treatment of Calu-3 cells with the furin inhibitor MI-1851 (10 μM) provided a 30- to 75-fold reduction in titers of infectious viruses in SARS-CoV-2 infected cells [4]. Furthermore, the simultaneous addition of the TMPRSS2 inhibitor MI-432 (50 μM) and the furin inhibitor MI-1851 (50 μM) reduced virus titers 10- to 32-fold compared to 50 μM of each inhibitor alone leading to a 100- to 250-fold decrease in SARS-CoV-2 multiplication (compared to untreated or DMSO treated cells). The elevated antiviral effect was also observed after the co-treatment of cells with the TMPRSS2 inhibitor MI-1900 and the furin inhibitor MI-1851 (caused five-fold reduction in viral titers compared to the cells treated with these inhibitors alone) [4]. The contribution of furin to the SARS-CoV-2 infection and pathogenesis was also supported by the characterization of the ΔPRRA mutant of the S protein, lacking the furin cleavage site. The ΔPRRA mutant reveals a lower replication in Calu3 cells due to the reduced spike protein processing compared to that of wild-type SARS-CoV-2. Therefore, it caused an attenuated disease in both hamster and K18-hACE2 transgenic mouse models of SARS-CoV-2 pathogenesis [23–25].

Previously, various 4-amidinobenzylamide-derived inhibitors were safely used to reduce the replication of numerous furin-dependent viruses *in vitro* in infected cells at concentrations up to 50 μM. The first generation of these substrate-analog furin inhibitors, containing three guanidine groups and one amidine, showed high lethality in mice within 1 h after intraperitoneal administration (5 mg/kg) [26]. To reduce the toxicity of these derivatives, their guanidine and amidine moieties were deleted or replaced, which considerably reduced the inhibitory effect on furin and consequently on the antiviral activity. In contrast, the replacement of the strongly basic arginine residues in P2 and P4

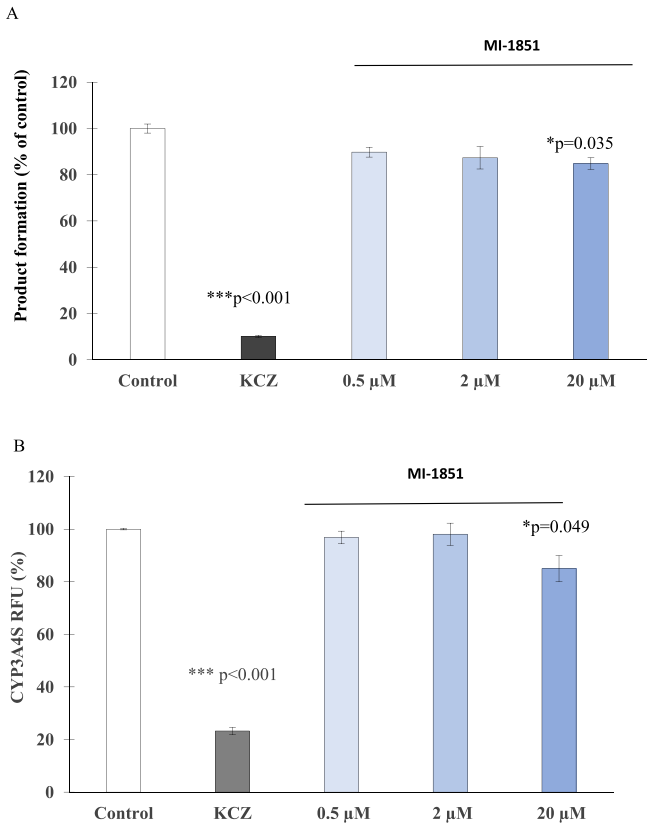

Fig. 4. Interaction of MI-1851 with human recombinant and microsomal CYP3A4. (A) Effects of inhibitor MI-1851 on 6β-hydroxytestosterone formation catalyzed by human recombinant CYP3A4, (B) and its impact on fluorescent product formation by human microsomal CYP3A4 isoenzyme. Human recombinant and microsomal CYP3A4 activities were only weakly inhibited by MI-1851 (*p = 0.035 and *p = 0.049 at 20 μM, respectively). Ketoconazole (KCZ) significantly decreased CYP3A4 activity in both assays (***p < 0.001; 1.0 μM KCZ was used in the recombinant CYP3A4 assay, while 5 μM in the assay with microsomes). Data represent product formation (% of control) ± SEM (n = 3) (A) and mean fluorescence intensity of CYP3A4 substrate (CYP3A4S RFU %) ± SEM (n = 3) (B).

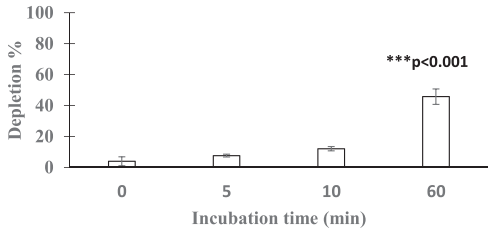

Fig. 5. Microsomal degradation of MI-1851. Stability assay of inhibitor MI-1851 during its incubation with human microsomes (0–60 min). Samples contained 50 μM MI-1851 with 0.7 mg/mL protein concentration in the assay buffer. Data represent mean depletion% values ± SEM (n = 3; ***p < 0.001).

positions with the less-basic canavanine (pK_a = 7.04) in inhibitor MI-1851 resulted in a more tolerable derivative. The canavanine side chains are almost completely protonated under slightly acidic conditions in the trans-Golgi network (at pH close to 6), leading to a nearly completely fourfold protonated inhibitor at P1, P2, P4 and P5 positions. In contrast, the canavanines are only partially protonated in the blood and extracellular space (at pH values above 7), thereby reducing the concentration of the fourfold protonated species. This property resulted in the significantly decreased toxicity in mice, which accepted an i.p. dose of 15 mg/kg MI-1851 [26]. After the i.p. administration of MI-1851

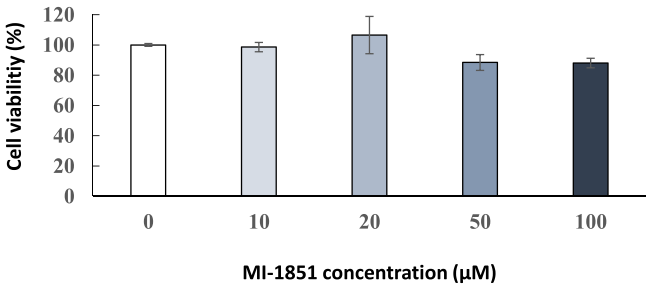

Fig. 6. Effects of MI-1851 on cell viability. Viability of PHHs after 24 h incubation with MI-1851 (expressed as % of control ± SEM). MI-1851 did not affect the cell viability up to 100 μM concentration (n = 3; p > 0.05).

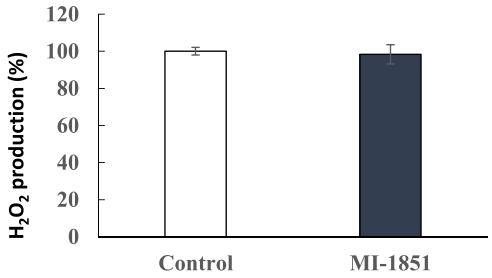

Fig. 7. Effects of MI-1851 on cellular H_2O_2 production. Lack of changes in the extracellular hydrogen peroxide levels after the 24 h treatment with MI-1851 (100 μM), based on the Amplex Red assays in PHHs. Data represent the mean H_2O_2 production (%) ± SEM (n = 3–6; p > 0.05).

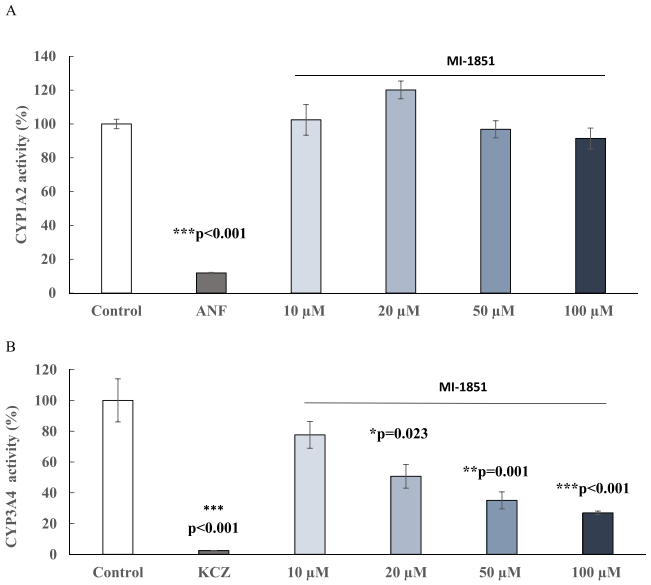

Fig. 8. Effects of MI-1851 on CYP1A2 and on CYP3A4 isoenzymes in PHHs. (A) MI-1851 did not affect the CYP1A2-mediated product formation. (B) Furin inhibitor decreased CYP3A4 activity at 20, 50 and 100 μM concentrations (*p = 0.023, **p = 0.001 and *** p < 0.001, respectively). The control inhibitors α-naphthoflavone (ANF) and ketoconazole (KCZ) showed significant inhibitory effects on CYP1A2 and CYP3A4, respectively (***p < 0.001). Data demonstrate the mean CYP activities (%) ± SEM (n = 3–4).

(2.5 mg/kg) to mice, its elimination half-life was 0.50 h with a peak plasma concentration (C_{max}) of approximately 3000 ng/mL (3.9 μM) [16].

Based on spectroscopic and ultrafiltration studies, inhibitor MI-1851 does not form stable complexes with HSA and it does not affect

significantly the albumin-binding of site I and site II ligands. Our previous investigation with benzamidine-derived inhibitors of trypsin-like serine proteases like compounds MI-432, MI-463, MI-482 and MI-1900 showed also no or only weak interactions with HSA [21]. Thus, it is reasonable to hypothesize that MI-1851 does not interfere with the albumin-binding of other medications.

In vitro pharmacokinetic properties of inhibitor MI-1851 such as its effects on CYP-mediated biotransformation pathways were also assessed in microsomal and hepatocyte-based models. In the microsomal stability assay, the significant decomposition of MI-1851 was observed leading to an approximately 45% decrease in its initial concentration (50 μM) after the 60 min incubation period.

In human microsomes, MI-1851 did not influence CYP1A2, 2C9, 2C19 and 2D6 activities. In contrast, the inhibition of CY3A4 was noticed in human recombinant CYP3A4 assay (20 μM), in human microsomes (20 μM) and in PHHs (20–100 μM). Nevertheless, in the *in vitro* assay with human recombinant CYP3A4, the furin inhibitor caused only slight inhibition of testosterone hydroxylation even at 20 μM concentration (Fig. 4 A), while other benzamidine derivatives tested previously (MI-432, MI-463, MI-482 and MI-1900) showed much stronger inhibitory effects (IC_{50} = 2–12 μM) [21]. These observations are also in agreement with the current experimental results (Fig. 4B) and the recently reported data [21] in regard to the microsomal CYP3A4 inhibition by MI-1851 and the other MI compounds listed. These findings suggest that MI-1851 is only a weak inhibitor of CYP3A4 and presumably it does not modify significantly the CYP3A4-mediated biotransformation of other drugs.

In vitro cytotoxicity tests revealed that MI-1851 can be safely used at 50 μM in cell cultures including human airway epithelial Calu-3 cells [4], human-like porcine-derived intestinal epithelial IPEC-J2 cells (supporting information), and PHHs as described in the present study. In addition, the lack of oxidative stress-inducing properties of inhibitor MI-1851 was also demonstrated. MI-1851 did not cause any changes in extracellular H_2O_2 production released from PHHs up to a concentration of 100 μM after 24 h treatment. These *in vitro* data support the good safety profile of inhibitor MI-1851, since it did not damage significantly hepatic, intestinal, and airway epithelial cells and did not exert deteriorating effect on redox homeostasis up to a concentration of 100 μM.

In conclusion, considering the *in vitro* impact of potential antiviral TMPRSS2 inhibitors on CYP3A4 [21,22], MI-1851 shows only a minimal safety risk from the perspective of drug-drug interaction. In addition, its negligible affinity to HSA and lack of cytotoxicity on PHHs and intestinal epithelial cells might indicate suitable *in vitro* pharmaco-toxicological parameters of this furin inhibitor. Nevertheless, further *in vivo* studies are reasonable to evaluate the PK/PD profile of MI-1851.

Author contributions

EPG designed the study. EPG and AST carried out CYP fluorometric and chemiluminescent experiments and evaluated data. TS was responsible for the design of inhibitor MI-1851 and provided this compound for the present study. PSZ completed UPLC-MS/MS measurements and data interpretation. EFN and MP performed spectroscopic studies and CYP3A4 assay with testosterone substrate. Statistical analysis was made by EPG. EPG, TS, and MP wrote the manuscript which was approved by the other authors.

Funding

This work was supported by the Hungarian National Research, Development and Innovation Office under grant number 124522 and by ÚNKP-21-5 New National Excellence Program of the Ministry for Innovation and Technology from the source of the National Research, Development and Innovation Fund.

Ethics declaration

Animal experiments were not carried out during this study.

CRediT authorship contribution statement

Erzsébet Pászti-Gere: Conceptualization, Methodology, Writing – original draft, Writing – review & editing, Funding aquisition, Supervision. **Anna Szentkirályi-Tóth:** Methodology, Data curation, Visualization. **Pál Szabó:** Methodology, Data curation, Validation, Resources. **Torsten Steinmetzer:** Conceptualization, Methodology, Writing – review & editing, Supervision. **Eszter Fliszár-Nyúl:** Methodology, Data curation, Visualization. **Miklós Poór:** Conceptualization, Methodology, Writing – review & editing, Funding aquisition, Supervision.

Conflict of interest statement

The work of this paper has been performed as independent scientific work with no interferences from any third party. The other authors declare that the research was conducted in the absence of any commercial or financial relationships that could be construed as a potential conflict of interest.

Acknowledgments

The authors thank to Katalin Fábián (Department of Pharmacology, Faculty of Pharmacy, University of Pécs, Pécs, Hungary) for her excellent assistance in the experimental work.

References

[1] M. Hoffmann, H. Hofmann-Winkler, S. Pöhlmann, Priming Time: How Cellular Proteases Arm Coronavirus Spike Proteins, in: E. Böttcher-Friebertshäuser, W. Garten, H. Klenk (Eds.), Activation of viruses by host proteases, Springer, Cham, 2018, pp. 71–98.

[2] E. Böttcher-Friebertshäuser, Membrane-Anchored Serine Proteases: Host Cell Factors in Proteolytic Activation of Viral Glycoproteins, in: E. Böttcher-Friebertshäuser, W. Garten, H. Klenk (Eds.), Activation of viruses by host proteases, Springer, Cham, 2018, pp. 153–203.

[3] R. Zang, M.F. Gomez Castro, B.T. McCune, Q. Zeng, P.W. Rothlauf, N.M. Sonnek, Z. Liu, K.F. Brulois, X. Wang, H.B. Greenberg, M.S. Diamond, M.A. Ciorba, S.P. J. Whelan, S. Ding, TMPRSS2 and TMPRSS4 promote SARS-CoV-2 infection of human small intestinal enterocytes, Sci. Immunol. 5 (47) (2020) eabc3582, https://doi.org/10.1126/sciimmunol.abc3582.

[4] D. Bestle, M.R. Heindl, H. Limburg, T. Van Lam van, O. Pilgram, H. Moulton, D. A. Stein, K. Hardes, M. Eickmann, O. Dolnik, C. Rohde, H.D. Klenk, W. Garten, T. Steinmetzer, E. Böttcher-Friebertshäuser, TMPRSS2 and furin are both essential for proteolytic activation of SARS-CoV-2 in human airway cells, Life Sci. Alliance 3 (9) (2020), e202000786, https://doi.org/10.26508/lsa.202000786.

[5] M. Hoffmann, H. Kleine-Weber, S. Schroeder, N. Krüger, T. Herrler, S. Erichsen, T. S. Schiergens, G. Herrler, N.H. Wu, A. Nitsche, M.A. Müller, C. Drosten, S. Pöhlmann, SARS-CoV-2 cell entry depends on ACE2 and TMPRSS2 and is blocked by a clinically proven protease inhibitor, Cell 181 (2) (2020) 271–280, https://doi.org/10.1016/j.cell.2020.02.052.

[6] M. Hoffmann, H. Kleine-Weber, S. Pöhlmann, A multibasic cleavage site in the spike protein of SARS-CoV-2 is essential for infection of human lung cells, Mol. Cell. 78 (4) (2020) 779–784, https://doi.org/10.1016/j.molcel.2020.04.022.

[7] G.L. Becker, F. Sielaff, M.E. Than, I. Lindberg, S. Routhier, R. Day, Y. Lu, W. Garten, T. Steinmetzer, Potent inhibitors of furin and furin-like proprotein convertases containing decarboxylated P1 arginine mimetics, J. Med. Chem. 53 (3) (2010) 1067–1075, https://doi.org/10.1021/jm9012455.

[8] H. Zhao, K.K.W. To, K.H. Sze, T.T. Yung, M. Bian, H. Lam, M.L. Yeung, C. Li, H. Chu, K.Y. Yuen, A broad-spectrum virus- and host-targeting peptide against respiratory viruses including influenza virus and SARS-CoV-2, Nat. Commun. 11 (2020) 4252, https://doi.org/10.1038/s41467-020-17986-9.

[9] H. Zhao, K.K.W. To, H. Lam, X. Zhou, J.F. Chan, Z. Peng, A.C.Y. Lee, J. Cai, W. M. Chan, J.D. Ip, C.C. Chan, M.L. Yeung, A.J. Zhang, A.W.H. Chu, S. Jiang, K. Y. Yuen, Cross-linking peptide and repurposed drugs inhibit both entry pathways of SARS-CoV-2, Nat. Commun. 12 (2021) 1517, https://doi.org/10.1038/s41467-021-21825-w.

[10] D. Schütz, Y.B. Ruiz-Blanco, J. Münch, F. Kirchhoff, E. Sanchez-Garcia, J.A. Müller, Peptide and peptide-based inhibitors of SARS-CoV-2 entry, Adv. Drug. Deliv. Rev. 167 (2020) 47–65, https://doi.org/10.1016/j.addr.2020.11.007.

[11] D.R. Owen, C.M.N. Allerton, A.S. Anderson, L. Aschenbrenner, M. Avery, S. Berritt, B. Boras, R.D. Cardin, A. Carlo, K.J. Coffman, A. Dantonio, L. Di, H. Eng, R. Ferre, K.S. Gajiwala, S.A. Gibson, S.E. Greasley, B.L. Hurst, E.P. Kadar, A.S. Kalgutkar, J. C. Lee, J. Lee, W. Liu, S.W. Mason, S. Noell, J.J. Novak, R.S. Obach, K. Ogilvie, N.

C. Patel, M. Pettersson, D.K. Rai, M.R. Reese, M.F. Sammons, J.G. Sathish, R.S. P. Singh, C.M. Steppan, A.E. Stewart, J.B. Tuttle, L. Updyke, P.R. Verhoest, L. Wei, Q. Yang, Y. Zhu, An oral SARS-CoV-2 M(pro) inhibitor clinical candidate for the treatment of COVID-19, Science 374 (6575) (2021) 1586–1593, https://doi.org/10.1126/science.abl4784.

[12] H.D. Klenk, W. Garten, Host cell proteases controlling virus pathogenicity, Trends Microbiol. 2 (2) (1994) 39–43, https://doi.org/10.1016/0966-842x(94)90123-6.

[13] N.G. Seidah, A. Prat, The biology and therapeutic targeting of the proprotein convertases, Nat. Rev. Drug. Discov. 11 (2012) 367–383, https://doi.org/10.1038/nrd3699.

[14] L. Du, Y. He, Y. Zhou, S. Liu, B.J. Zheng, S. Jiang, The spike protein of SARS-CoV–a target for vaccine and therapeutic development, Nat. Rev. Microbiol. 7 (2009) 226–236, https://doi.org/10.1038/nrmicro2090.

[15] Y.W. Cheng, T.L. Chao, C.L. Li, M.F. Chiu, H.C. Kao, S.H. Wang, Y.H. Pang, C. H. Lin, Y.M. Tsai, W.H. Lee, M.H. Tao, T.C. Ho, P.Y. Wu, L.T. Jang, P.J. Chen, S. Y. Chang, S.H. Yeh, Furin inhibitors block SARS-CoV-2 spike protein cleavage to suppress virus production and cytopathic effects, Cell. Rep. 33 (2) (2020), 108254, https://doi.org/10.1016/j.celrep.2020.108254.

[16] T.V. Lam van, M.R. Heindl, C. Schlutt, E. Böttcher-Friebertshäuser, R. Bartenschlager, G. Klebe, H. Brandstetter, S.O. Dahms, T. Steinmetzer, The basicity makes the difference: improved canavanine-derived inhibitors of the proprotein convertase furin, ACS Med. Chem. Lett. 12 (3) (2021) 426–432, https://doi.org/10.1021/acsmedchemlett.0c00651.

[17] Z. Faisal, B. Lemli, D. Szerencsés, S. Kunsági-Máté, M. Bálint, C. Hetényi, M. Kuzma, M. Mayer, M. Poór, Interactions of zearalenone and its reduced metabolites α-zearalenol and β-zearalenol with serum albumins: species differences, binding sites, and thermodynamics, Mycotoxin Res. 34 (2018) 269–278, https://doi.org/10.1007/s12550-018-0321-6.

[18] Z. Faisal, V. Mohos, E. Fliszár-Nyúl, K. Valentová, K. Káňová, B. Lemli, S. Kunsági-Máté, M. Poór, Interaction of silymarin components and their sulfate metabolites with human serum albumin and cytochrome P450 (2C9, 2C19, 2D6, and 3A4) enzymes, Biomed. Pharmacother. 138 (2021), 111459, https://doi.org/10.1016/j.biopha.2021.111459.

[19] V. Mohos, E. Fliszár-Nyúl, G. Schilli, C. Hetényi, B. Lemli, S. Kunsági-Máté, B. Bognár, M. Poór, Interaction of chrysin and its main conjugated metabolites chrysin-7-sulfate and chrysin-7-glucuronide with serum albumin, Int. J. Mol. Sci. 19 (12) (2018) 4073, https://doi.org/10.3390/ijms19124073.

[20] E. Fliszár-Nyúl, B. Lemli, S. Kunsági-Máté, L. Dellafiora, C. Dall'Asta, G. Cruciani, G. Pethő, M. Poór, Interaction of mycotoxin alternariol with serum albumin, Int. J. Mol. Sci. 20 (9) (2019) 2352, https://doi.org/10.3390/ijms20092352.

[21] E. Pászti-Gere, A. Szentkirályi, G. Zs. Fedor, Z. Nagy, Z. Szimrók, A. Pászti, O. Pászti, T. Pilgram, S. Steinmetzer, E. Bodnárová, M.Poór Fliszár-Nyúl, In vitro interaction of potential antiviral TMPRSS2 inhibitors with human serum albumin and cytochrome P 450 isoenzymes, Biomed. Pharmacother. 146 (2022), 112513, https://doi.org/10.1016/j.biopha.2021.112513.

[22] E. Pászti-Gere, J. Pomothy, Á. Jerzsele, O. Pilgram, T. Steinmetzer, Exposure of human intestinal epithelial cells and primary human hepatocytes to trypsin-like serine protease inhibitors with potential antiviral effect, J. Enzym. Inhib. Med. Chem. 36 (1) (2021) 659–668, https://doi.org/10.1080/14756366.2021.1886093.

[23] B.A. Johnson, X. Xie, B. Kalveram, K.G. Lokugamage, A. Muruato, J. Zou, X. Zhang, T. Juelich, J.K. Smith, L. Zhang, N. Bopp, C. Schindewolf, M. Vu, A. Vanderheiden, D. Swetnam, J.A. Plante, P. Aguilar, K.S. Plante, B. Lee, S.C. Weaver, M.S. Suthar, A.L. Routh, P. Ren, Z. Ku, Z. An, K. Debbink, P.Y. Shi, A.N. Freiberg, V. D. Menachery, Furin cleavage site is key to SARS-CoV-2 pathogenesis, bioRxiv (2020), 268854, https://doi.org/10.1101/2020.08.26.268854.

[24] B.A. Johnson, X. Xie, A.L. Bailey, B. Kalveram, K.G. Lokugamage, A. Muruato, J. Zou, X. Zhang, T. Juelich, J.K. Smith, L. Zhang, N. Bopp, C. Schindewolf, M. Vu, A. Vanderheiden, E.S. Winkler, D. Swetnam, J.A. Plante, P. Aguilar, K.S. Plante, B. Lee, C.S. Weaver, M.S. Suthar, A.L. Routh, P. Ren, Z. Ku, Z. An, K. Debbink, M. S. Diamond, P.Y. Shi, A.N. Freiberg, V.D. Menachery, Loss of furin cleavage site attenuates SARS-CoV-2 pathogenesis, Nature 591 (2021) 293–299, https://doi.org/10.1038/s41586-021-03237-4.

[25] M. Sasaki, S. Toba, Y. Itakura, H.M. Chambaro, M. Kishimoto, K. Tabata, K. Intaruck, K. Uemura, T. Sanaki, A. Sato, W.W. Hall, Y. Orba, H. Sawa, SARS-CoV-2 bearing a mutation at the S1/S2 cleavage site exhibits attenuated virulence and confers protective immunity, mBio 12 (4) (2021), e0141521, https://doi.org/10.1128/mBio.01415-21.

[26] T. Ivanova, K. Hardes, S. Kallis, S.O. Dahms, M.E. Than, S. Künzel, E. Böttcher-Friebertshäuser, I. Lindberg, G.S. Jiao, R. Bartenschlager, T. Steinmetzer, Optimization of substrate-analogue furin inhibitors, ChemMedChem 12 (23) (2017) 1953–1968, https://doi.org/10.1002/cmdc.201700596.